

SUPPLEMENTAL DATA

SUPPLEMENTAL VIDEO LEGENDS

Supplemental Video 1. SDF-1 α induces rapid CD4 $^{+}$ T cell migration.

Freshly isolated human CD4 $^{+}$ T cells were placed into fibronectin-coated glass-bottom dishes in a temperature-controlled (37°C) stage incubator and the response to stimulation with SDF-1 α (100 ng/ml) was monitored by video microscopy. SDF-1 α was added after 10 min. Leica DMI6000B microscope, 63x oil objective (NA 1.4), frame rate: 12 frames per min.

Supplemental Video 2. CBX blocks the rapid ATP release in response to SDF-1 α .

Freshly isolated CD4 $^{+}$ T cells were stained with the cell-surface targeting ATP indicator 2-2Zn and ATP release following treatment with SDF-1 α (100 ng/ml; left) or CBX (100 μ M) and SDF-1 α (right) was recorded by video fluorescence microscopy. Leica DMI6000B microscope, 100x oil objective (NA 1.4), frame rate: 20 frames per min; scale bar: 5 μ m.

Supplemental Video 3. T cell migration depends on pannexin-1.

Jurkat cells were transfected with siRNA targeting pannexin-1 (PANX1) or a non-targeting control siRNA. 48 h later, cells were placed into fibronectin-coated glass-bottom dishes and migration in the presence or absence of SDF-1 α (100 ng/ml) was observed by video microscopy. Cells were tracked by ImageJ software. Leica DMIR microscope, 20x objective (NA 0.4), frame rate: 1.33 frames per min.

Supplemental Video 4. Mitochondrial ATP fuels pseudopod formation.

CD4 $^{+}$ T cells were stained with the ATP probe 2-2Zn and the mitochondrial Ca $^{2+}$ probe Rhod-2, stimulated with SDF-1 α (100 ng/ml) and immediately observed by time-lapse fluorescence microscopy. Leica DMI6000B microscope, 100x oil objective, frame rate: 30 frames per min.

Supplemental Video 5. P2X4 receptors regulate SDF-1 α -dependent Ca $^{2+}$ signaling.

CD4 $^{+}$ T cells were loaded with Fluo-4, treated with 5-BDBD (P2X4 antagonist; 10 μ M) or vehicle (control) and the change in cytosolic Ca $^{2+}$ following stimulation with SDF-1 α (100 ng/ml; added after 1 min) was monitored by fluorescence microscopy. Leica DMI6000B microscope, 40x objective (NA 0.75), frame rate: 20 frames per min.

Supplemental Video 6. P2X4 receptors promote cell polarization and migration in Jurkat cells and CD4⁺ T lymphoblasts.

Jurkat cells were transfected with siRNA targeting P2X4 receptors or a non-targeting control siRNA. 48 h later, cells were placed into fibronectin-coated glass-bottom dishes and migration in the presence or absence of SDF-1 α (100 ng/ml) was observed by video microscopy. CD4⁺ T cells were stimulated with anti-CD3/anti-CD28 antibody coated beads for 3 days, attached to fibronectin-coated glass-bottom dishes and treated for 10 min with culture medium (control) or the P2X4 receptor antagonist 5-BDBD (10 μ M) before imaging was started. Leica DMIIR microscope, 20x objective (NA 0.4), frame rate: 1.33 frames per min.

Supplemental Video 7. P2X4 receptors accumulate with mitochondria at the leading edge of moving cells.

Jurkat cells expressing EGFP-tagged P2X4 receptors and stained with MitoTracker Red CM-H2Xros were imaged in the presence or absence of SDF-1 α (100 ng/ml). Leica DMI6000B microscope, 100x oil objective, frame rate: 20 frames per min.

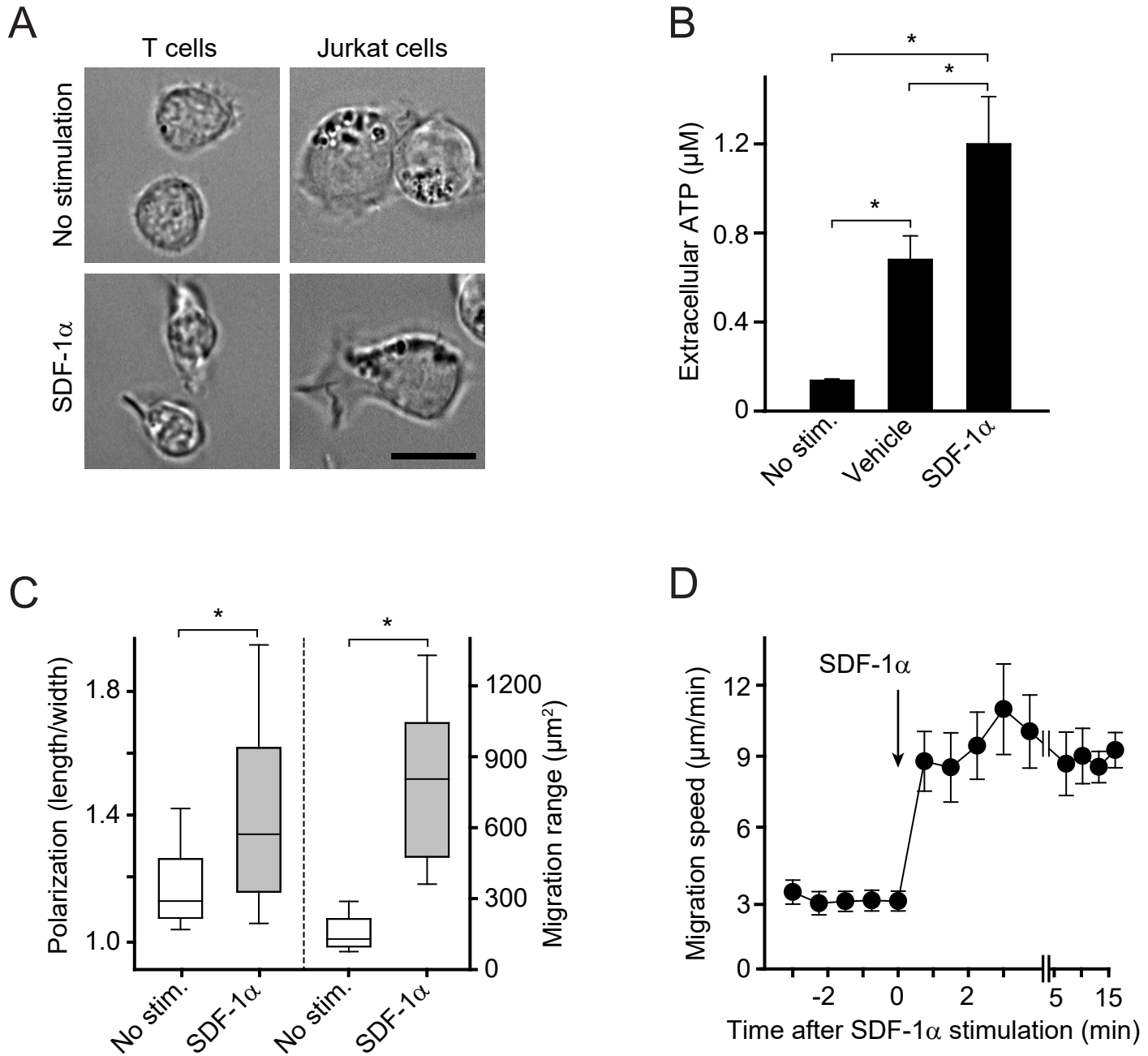
Supplemental Video 8. Mitochondrial distribution defines the mode of T cell migration.

CD4⁺ T cells were stimulated for 3 days with anti-CD3/anti-CD28 antibody-coated beads, attached to fibronectin-coated glass-bottom dishes and stained with MitoTracker Red CM-H2Xros. Migration and mitochondrial localization were observed by fluorescence and bright field time-lapse microscopy. Mitochondria accumulate mostly in the back of fast-moving cells and move to the front of cells probing their environment or interacting with other cells. Leica DMI6000B microscope, 63x oil objective (NA 1.4), frame rate: 6 frames per min.

Supplemental Video 9. P2X4 receptors maintain mitochondrial activity.

CD4⁺ T cells were stimulated for 3 days with anti-CD3/anti-CD28 antibody-coated beads, attached to fibronectin-coated glass-bottom dishes and stained with MitoTracker Red CM-H2Xros. Migration and mitochondrial localization were observed by fluorescence and bright field time-lapse microscopy. The P2X4 receptor inhibitor 5-BDBD (10 μ M) or medium (control) were added after 1 min. The calibration bar indicates the range of fluorescence intensities. Leica DMI6000B microscope, 63x oil objective (NA 1.4), frame rate: 6 frames per min.

Supplemental Figure 1

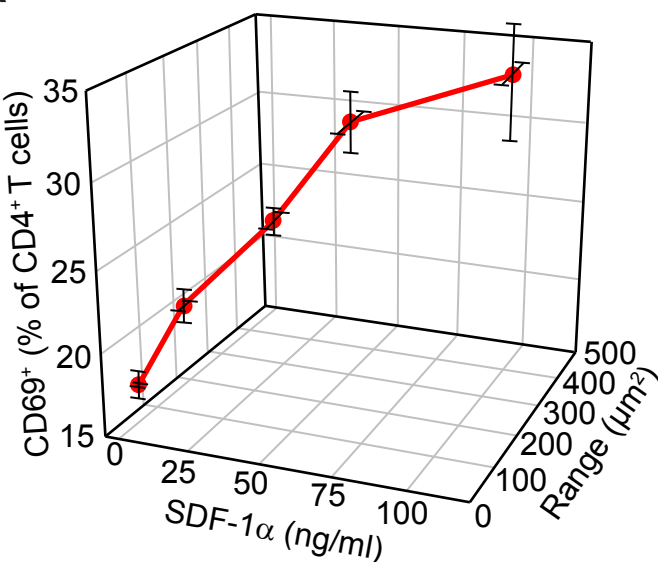


Supplemental Figure 1. SDF-1 α induces ATP release, cell polarization, and migration in primary CD4 $^{+}$ T cells and Jurkat cells.

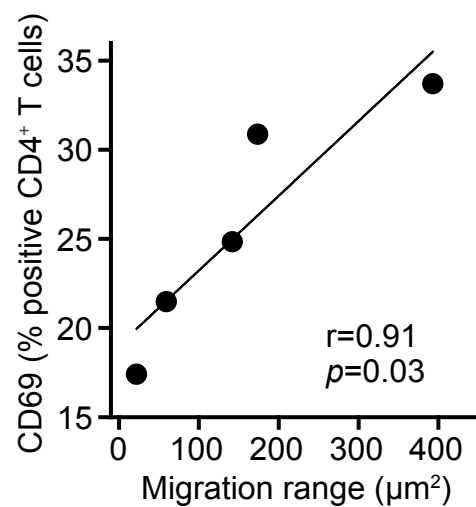
A Polarization of primary human CD4 $^{+}$ T cells and Jurkat cells following stimulation with SDF-1 α . Images representative of at least 200 cells demonstrating the change in cell shape 5 min after addition of SDF-1 α (100 ng/ml) are shown; 63x objective; scale bar: 10 μ m. **B** ATP concentrations in the supernatants of untreated, vehicle-treated or SDF-1 α stimulated (5 min) Jurkat cells (mean \pm SD, n=3, *p<0.05; one-way ANOVA). **C-D** Cell polarization, migration range (**C**) and migration speed (**D**) of Jurkat cells stimulated with SDF-1 α and observed with video microscopy for 30 min. Box plots (**C**) show the distribution of n=150 cells analyzed in 3 separate experiments; *p<0.05 (Mann-Whitney U test). Data in **D** represent mean \pm SD of n=40 cells analyzed in one experiment and are representative of n=12 experiments with similar results.

Supplemental Figure 2

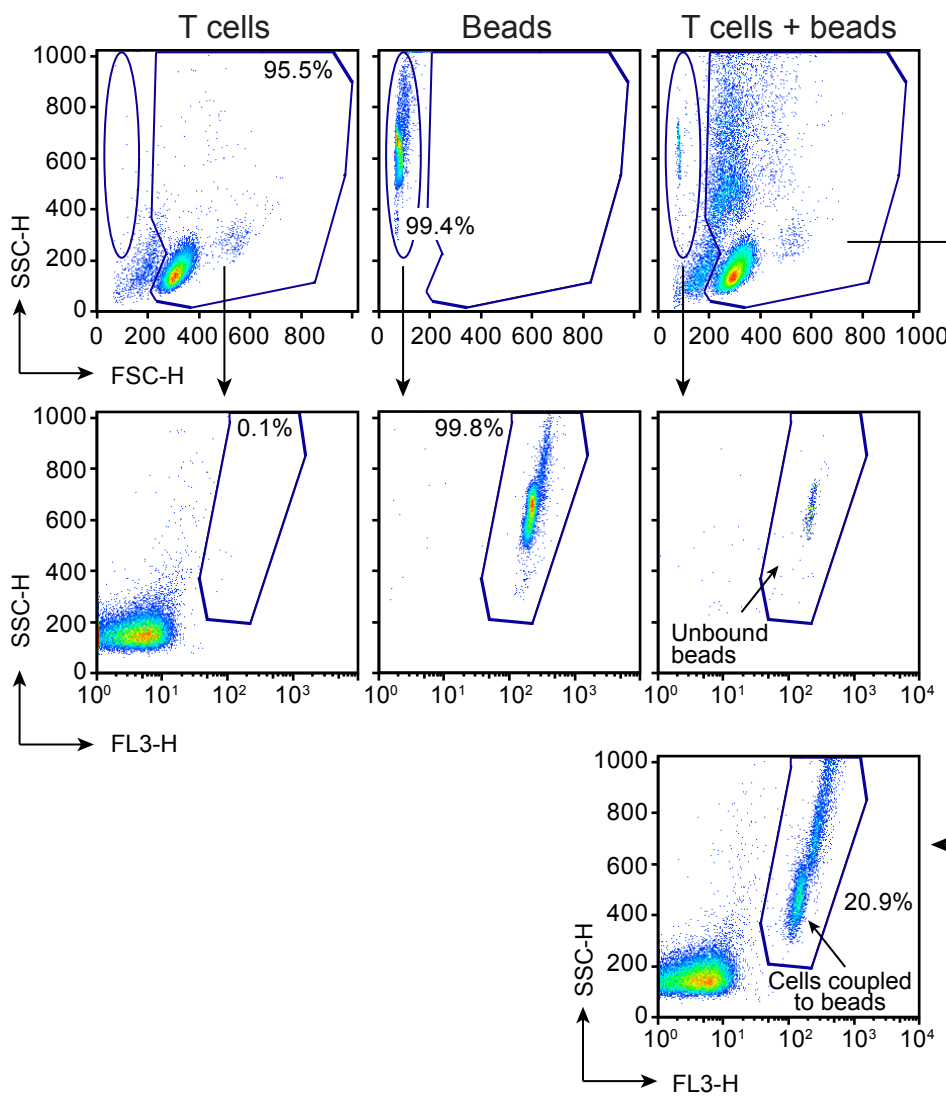
A



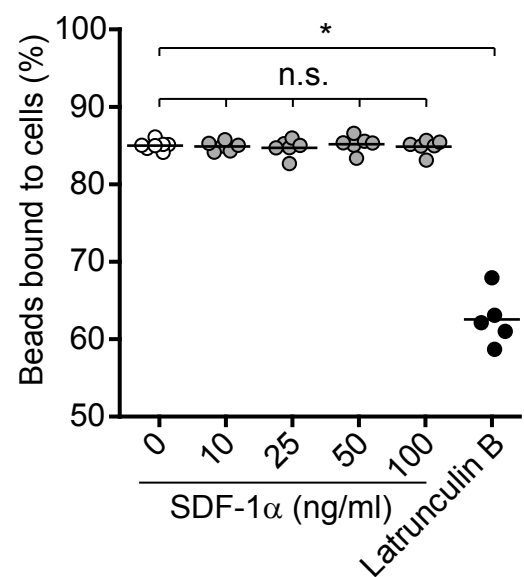
B



C



D



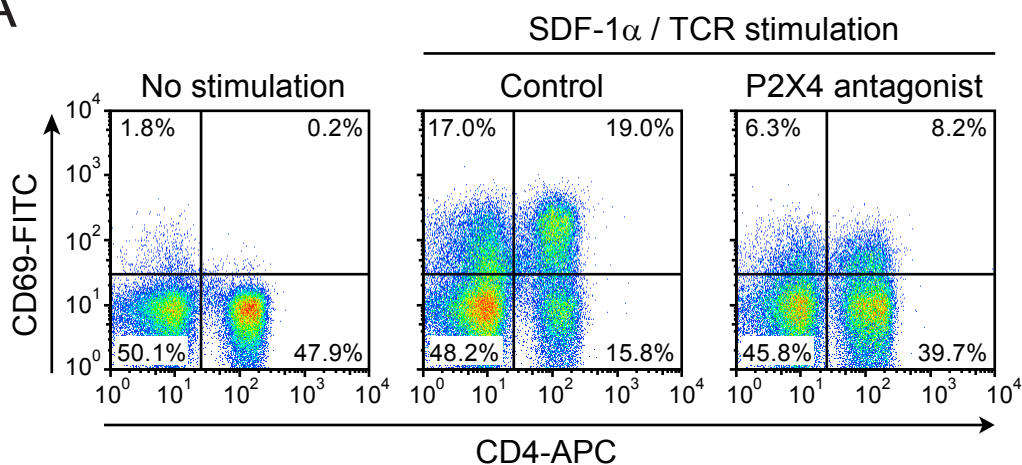
Supplemental Figure 2. SDF-1 α promotes T cell activation by enhancing T cell migration.

A PBMCs were placed into fibronectin-coated glass-bottom chamber slides, stained with APC-labeled anti-CD4 antibodies, stimulated with SDF-1 α at the indicated concentrations and migration of CD4 $^+$ T cells was tracked by time-lapse microscopy for 30 min. The area the cells covered (migration range) was calculated with ImageJ. Data are mean \pm SD of n=50 cells analyzed in 3 separate experiments. CD69 expression in CD4 $^+$ T cells following stimulation with increasing concentrations of SDF-1 α and anti-CD3 antibodies in a PBMC culture for 5 h was analyzed by flow cytometry. Data represent mean \pm SD of n=3 separate experiments. **B** Correlation between CD69 expression and migration speed. Data are the mean values of the experiments shown in **A**; r: Pearson's correlation coefficient. **C-D** CD4 $^+$ T cells were incubated with anti-CD3/anti-CD28 antibody-coated microbeads in microcentrifuge tubes in the presence or absence of increasing concentrations of SDF-1 α or latrunculin B (10 μ g/ml) for 15 min and coupling of T cells to beads was determined by flow cytometry by calculating the number of beads bound to cells. Representative dot blots demonstrating the gating strategy used to identify free and bound beads is shown in **C**. Results of n=5 (latrunculin B), 6 (SDF-1 α treated samples), or 7 (control) independent experiments are shown in **D**. Latrunculin B, an inhibitor of immune synapse formation, was included as a negative control to define passive binding to beads.

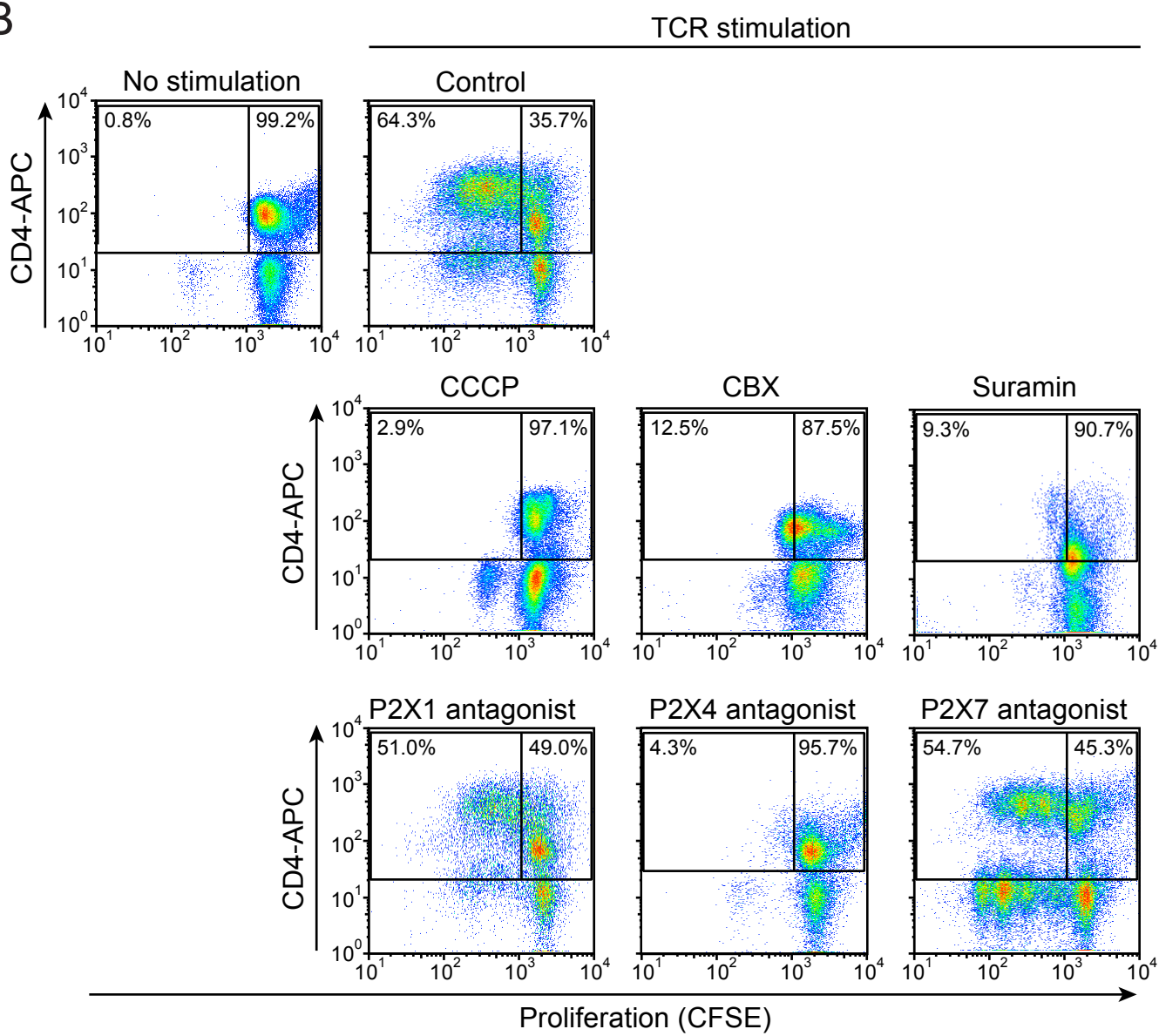
*p<0.05 (one-way ANOVA); n.s., not significant.

Supplemental Figure 3

A



B

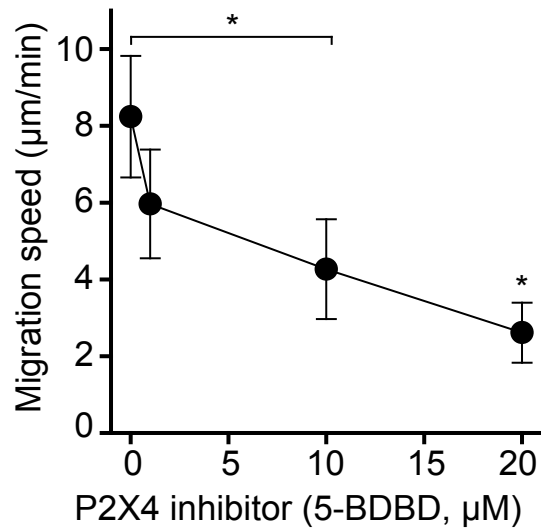


Supplemental Figure 3. Inhibition of T cell migration by blocking autocrine purinergic signaling prevents CD4⁺ T cell activation.

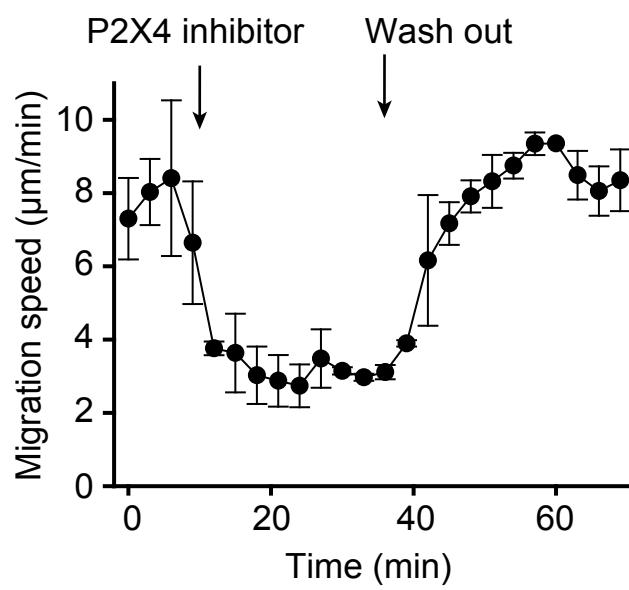
A CD69 expression was determined in unstimulated CD4⁺ T cells and in CD4⁺ T cells stimulated for 5 h with SDF-1 α and anti-CD3 antibodies in a PBMC culture in the presence or absence (control) of 5-BDBD (10 μ M; P2X4 antagonist). **B** Proliferation of CD4⁺ T cells was measured after stimulating PBMCs for 72 h with soluble anti-CD3 antibodies in the presence or absence of CCCP (5 μ M), CBX (100 μ M), suramin (100 μ M), or inhibitors of P2X1 (NF023; 10 μ M), P2X4 (5-BDBD; 10 μ M), and P2X7 (A438079; 1 μ M) receptors. Plots are representative of n=6 (**A**) or 3 (**B**) independent experiments. TCR: T cell receptor.

Supplemental Figure 4

A



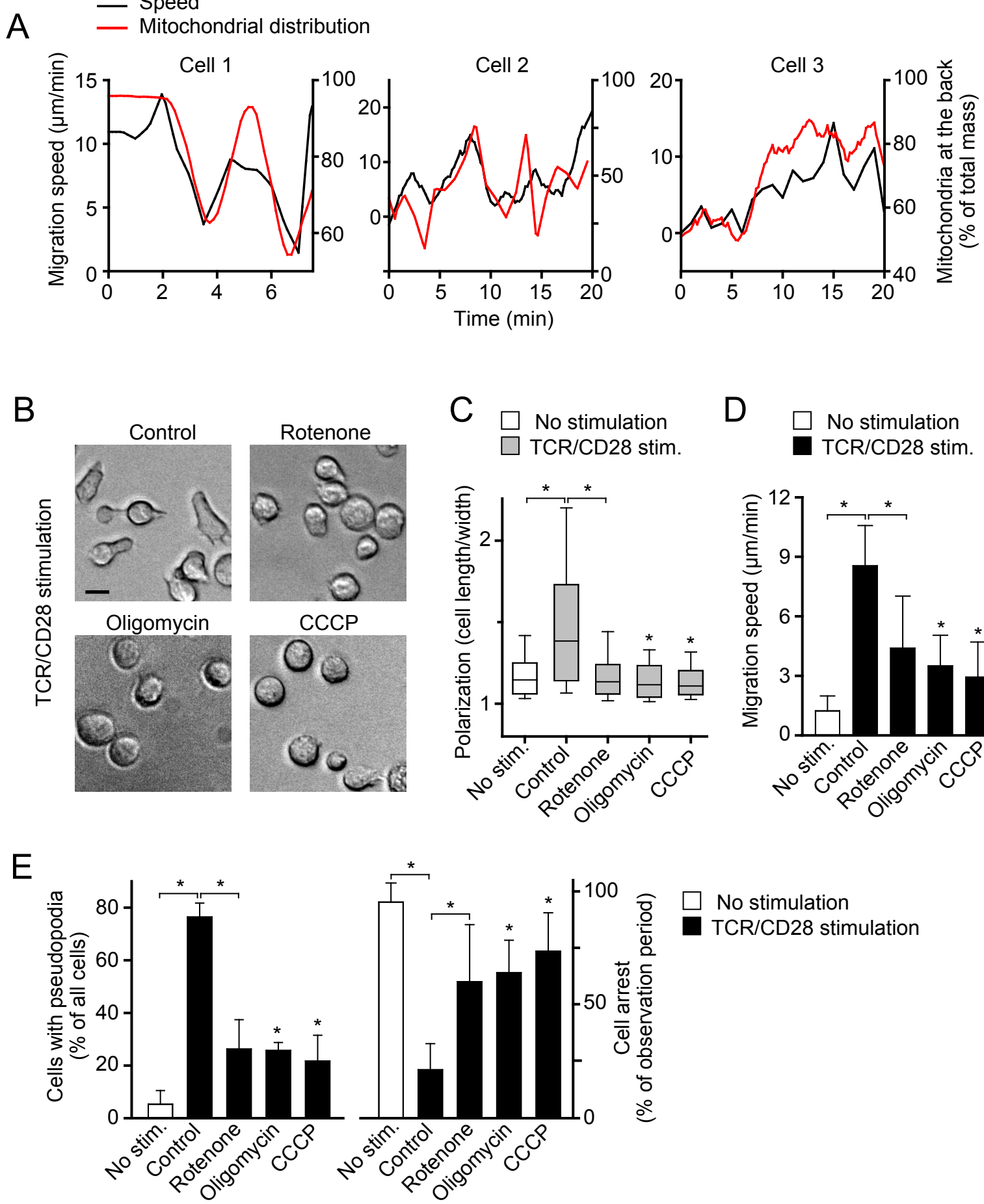
B



Supplemental Figure 4. P2X4 receptor inhibition with 5-BDBD reversibly blocks T cell migration.

A CD4⁺ T cells stimulated for 3 days with anti-CD3/anti-CD28 antibody-coated microbeads were treated with the indicated concentrations of the P2X4 antagonist 5-BDBD and migration speed was analyzed by time-lapse microscopy. Data show mean values \pm SD of n=5 experiments each comprising n=40 cells; * p <0.05 vs. control (one-way ANOVA). **B** CD4⁺ T lymphoblasts were attached to fibronectin-coated glass-bottom dishes, placed into a temperature-controlled (37°C) stage incubator and bright field images were captured at 45 s intervals. At the indicated time point (t=15 min), 5-BDBD (10 μ M) was added. At t=45 min, 5-BDBD was washed out and motility was observed for another 15 min. Data represent mean \pm SD of n=80 cells analyzed in n=2 experiments.

Supplemental Figure 5

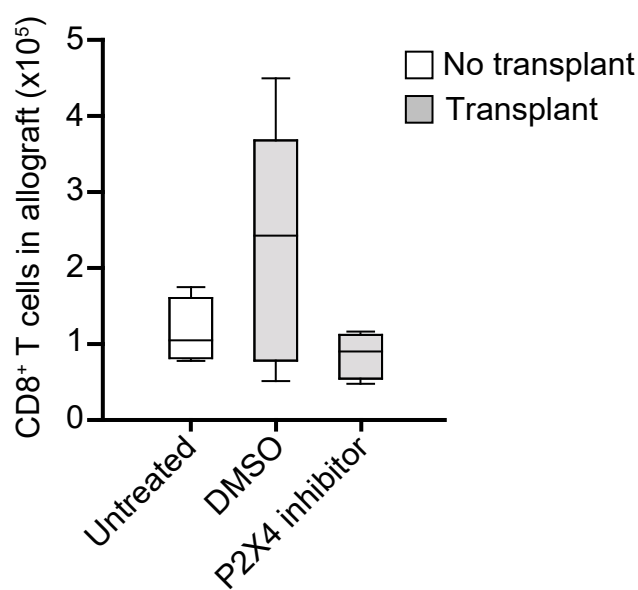


Supplemental Figure 5. Mitochondria regulate cell polarization and migration of T cells.

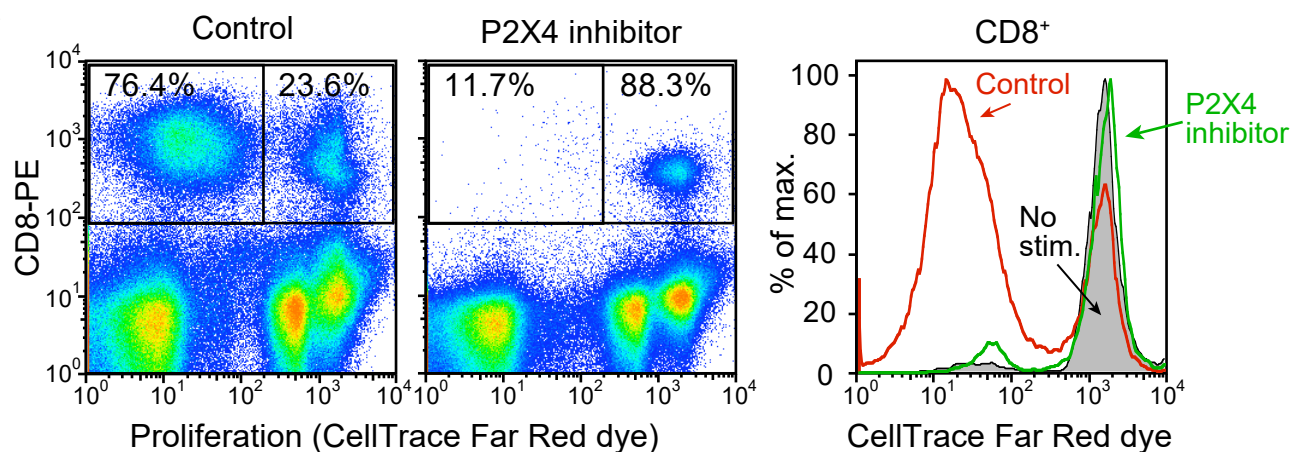
A CD4⁺ T cell lymphoblast were stained with MitoTracker Red CM-H2Xros. Cells were observed with live-cell fluorescence and bright field microscopy. Images were captured at a frame rate of 6 per min and migration speed and localization of mitochondria were analyzed in 30 s increments. Representative traces of 3 out of 10 cells analyzed are shown. **B-E** CD4⁺ T cell lymphoblasts were treated with the mitochondrial inhibitors rotenone (1 μ M), oligomycin (1 μ M) and CCCP (1 μ M) for 10 min and observed with video microscopy for 30 min. Representative images demonstrating rounded cell shapes in inhibitor-treated cells are shown in **B** (20x objective; scale bar: 10 μ m). The effect of mitochondrial inhibition on cell polarization (**C**), migration speed (**D**), pseudopod formation and the time cells were not moving during the observation period (**E**) were analyzed. Box plots in **C** show the distribution of n=265 (no stimulation), 95 (control), 93 (rotenone), 105 (oligomycin) and 155 (CCCP) cells derived from n=3 or 5 (no stimulation) individual experiments. *p<0.05 vs. control (Kruskal-Wallis test). Data in **D** and **E** are mean values \pm SD of n=5 (no stimulation), 7 (control), 4 (CCCP, rotenone), and 3 (oligomycin) separate experiments each comprising n=20-40 cells. *p<0.05 vs. control, one-way ANOVA; TCR: T cell receptor.

Supplemental Figure 6

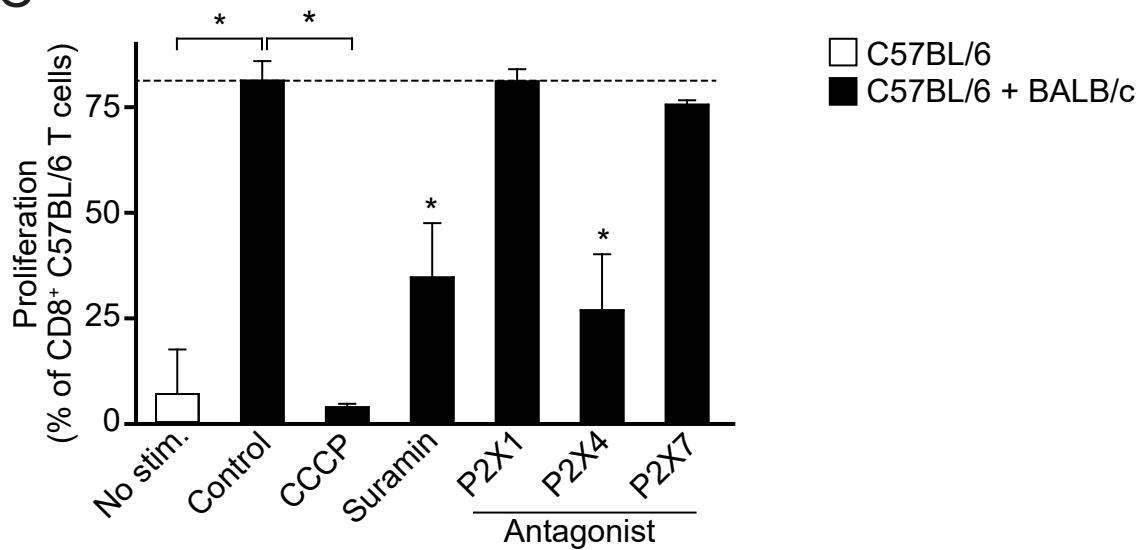
A



B



C



Supplemental Figure 6. P2X4 receptor inhibition blocks migration of CD8⁺ T cells into lung allografts and reduces in vitro proliferation in mixed lymphocyte reactions.

A Recipient C57BL/6 mice were treated with the P2X4 inhibitor 5-BDBD or vehicle (DMSO) 24 h before and immediately after transplantation of BALB/c lung allografts. The number of CD8⁺ T cells infiltrating the lung allograft was determined 24 h after transplantation by flow cytometry; n=4 (non-transplanted control and P2X4 inhibitor-treated group) or n=6 (DMSO-treated group).

B-C In vitro proliferation of C57BL/6 CD8⁺ T cells (responders) co-cultured in a mixed lymphocyte reaction with BALB/c splenocytes (stimulators) in the presence or absence of CCCP (1 μ M), suramin (100 μ M), NF279 (P2X1 antagonist; 20 μ M), 5-BDBD (P2X4 antagonist; 20 μ M), or A438079 (P2X7 antagonist; 20 μ M) for 4 days. Representative dot plots (**B**) and averaged results (mean \pm SD; **C**) of n=3 separate experiments are shown; *p<0.05 vs. control (one-way ANOVA).